Comparison of multiple sclerosis lesions segmentation using quantitative or FLAIR MR images

Vandeleene N.[1], Lommers E.[1, 2], Maquet P.[1, 2], Phillips C.[1]

[1] GIGA CRC *in vivo* imaging [2] Clinical Neuroimmunology Unit, Neurology Department, CHU Liege; University of Liege, Belgium

INTRODUCTION

FLAIR sequence from conventional MRI is the most commonly used imaging technique for the diagnosis and follow-up of multiple sclerosis (MS) disease though it has limited histopathological specificity. "Quantitative MRI" (qMRI), as opposed to conventional MRI, provides quantitative measures of brain tissues and should improve the characterization of lesioned tissues. With a multi-parameter mapping (MPM) protocol, 4 parameter maps are constructed (MTsat, PD, R1 and R2*), reflecting tissues physical properties associated to biological features such as water, iron and myelin content [1]. This makes qMRI a good candidate for finer characterization of MS lesions [2, 3]. We investigated whether MPM mapping can improve lesions segmentation based on information gained by these 4 parameters.

METHODS

Thirty-six patients were recruited at the specialized MS outpatient clinic of the Liège University Hospital, Belgium. MRI data were acquired either on a 3T Allegra or Prisma MRI scanner. MRI acquisitions included an MPM protocol, consisting of 3 co-localized 3D multi-echo FLASH acquisitions at 1x1x1 mm³ resolution and 2 additional calibration sequences to correct for inhomogeneities in the RF transmit field. A FLAIR sequence was also recorded with spatial resolution of 1x1x1 mm³ [4].

Two lesion masks were generated, based on FLAIR images on one side (mask A) and MPM maps on the other (mask B). Mask A is derived from the FLAIR image using the LST toolbox [5], further corrected by an expert. Mask B is obtained from the segmentation of the MPM maps by the US-with-Lesion tool [6, 7], initialized with mask A. We isolated individual lesions and matched them within both masks. Four different sub-regions were defined **(Figure 1)**:

- The intersection between lesions from both masks ($A \cap B$),
- The region only in FLAIR-derived mask ($A \setminus B$),
- The region only in MPM-derived mask ($B \setminus A$),
- The region of normal-appearing white matter (NAWM).

For each lesion individually in each subject, we extracted the voxels median value from the 4 sub-regions, in the 4 parametric maps (MTsat, PD, R1, R2*) and in the FLAIR intensities. We considered that the intersection region $A \cap B$, where the two masks are in agreement, contains the voxels that are the most likely to actually correspond to lesions as classically defined. The NAWM region represents the reference parameter distribution in tissues classified as “healthy” around the lesions. To generate this distribution, the same number of voxels were randomly chosen in the white matter tissue extracted from all subjects, for each parameter. The distributions of data in the four sub-regions were compared to each other, individually for each parameter. Statistical significance was evaluated with ANOVA tests.

Figure 1: Configuration of the different sub-regions used for statistical tests

The two masks (FLAIR-based and MPM-based) are compared to each other and four regions are specified: the intersection region $A \cap B$, the region with FLAIR only $A \setminus B$, the region with MPM only $B \setminus A$, and the region of NAWM (not depicted in the diagram). The median of MPM parameters will be extracted in those regions.
On average over all lesions and subjects, the two regions $A \setminus B$ and $B \setminus A$ constitute a two-mm³-thick layer around the intersection region, not regarding the lesion size.

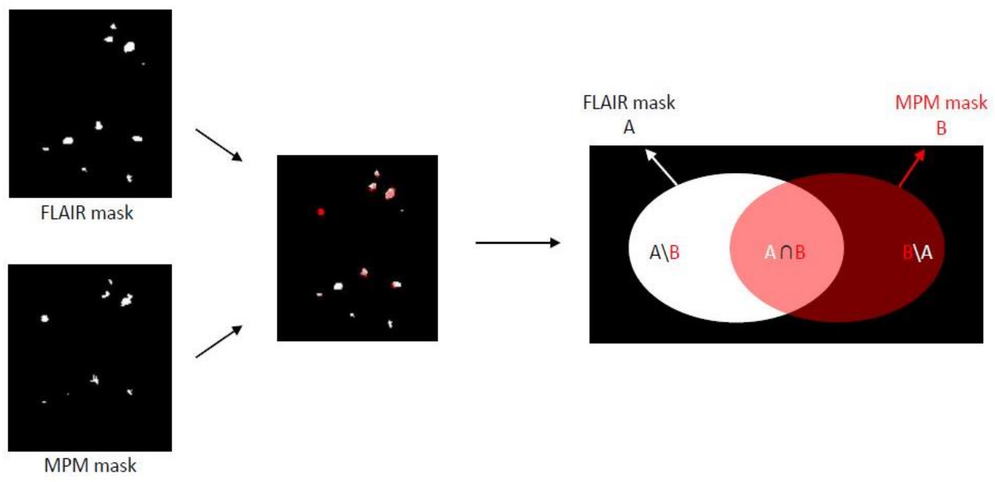

Figure 2: Violin plots of the median voxels values in all lesions from all subjects, comparing sub-regions and parameters (MT, PD, R1, R2* and FLAIR intensities)

For MT, PD and R1, region $B \setminus A$ is closer to the intersection region, while region $A \setminus B$ is closer to the reference healthy tissue (NAWM). The same behavior appears for R2*, although a little bit less pronounced. Such observations cannot be made for FLAIR intensities.

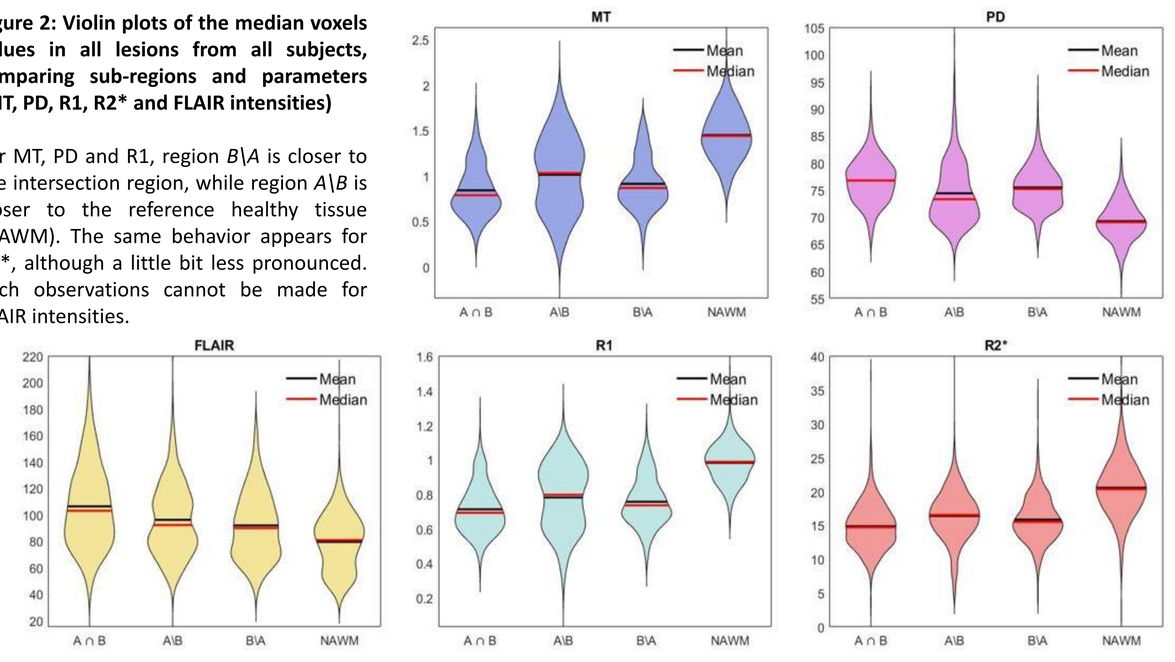

RESULTS

The MPM-based mask is generated with the corresponding FLAIR-based mask as an a priori, established from multi-channel MPM data comprising MT, PD and R1. R2* was excluded due to its noisy nature and low specificity to MS lesions. The two available masks are quite similar, with a Dice score of 0.6246 among the subjects. On average over all lesions and subjects, regions $A \setminus B$ and $B \setminus A$ constitute a two-mm³-thick layer around the intersection region, independently of the lesion size. This number was determined by counting the number of 1 voxel erosion steps needed for the region ($A \setminus B$ or $B \setminus A$) to disappear.

Violin plots **(Figure 2)**, show across all patients that for each MPM parameter, region $B \setminus A$ is closer to region $A \cap B$ than $A \setminus B$. Moreover region $A \setminus B$ is closer to the NAWM values than $B \setminus A$. This suggests that MPM-derived lesion masks are more specific than the FLAIR-derived masks, because they capture voxels with a data distribution closer to the intersection one, thus more likely to detect actual lesioned tissue. However, for FLAIR intensities, the contrary is observed: region $A \setminus B$ is closer to the intersection region, while region $B \setminus A$ is moving towards NAWM.

The high variability of voxel values in the $A \setminus B$ violin distribution, almost in the shape of a bimodal Gaussian distribution, suggests that some voxels are correctly classified as lesion, while others are more likely to indicate NAWM. Such spreading appears for the 4 parametric maps (although a little bit less pronounced in R2* map) but not for the FLAIR intensities. Voxels in the $A \setminus B$ and $B \setminus A$ regions with values close to those of the NAWM are very likely misclassified voxels. Indeed, by plotting the histograms of values in each region, there is an important overlap between regions *A/B* and NAWM, which is not very apparent for region *B/A,* much closer to the intersection distribution. Still this indicates that multi-parametric maps bring information about the lesioned tissues which is not available in the FLAIR intensities and likely leads to a more realistic description of the lesioned tissue.

CONCLUSION

Our results show that conducting segmentation of MS lesions using quantitative maps rather than FLAIR images allows to capture more voxels likely to be lesions, which could not be captured in FLAIR. However, the voxels considered as lesions in FLAIR are closer to normal appearing white matter, which could mean that those voxels result from an artefact or a wrong segmentation decision. Histopathological study of MS brains would allow to assess this outcome, by comparing the true lesion histopathological segmentation, and determine whether or not MPM maps segmentation gives better results than in FLAIR data [8].
In addition to indicating a more accurate lesion delineation in multi-parametric maps, this whole method helps to advertise the Unifed Segmentation with Lesion (USwL) technique recently developed. Indeed, the MPM-based mask was generated from USwL, which requires an a priori mask, in this case the FLAIR-based mask was selected. In some way, USwL seems to be correcting the input mask and producing a finer segmentation of lesions.
To conclude, the usage of both MPM maps over FLAIR images and the advanced USwL algorithm for segmentation leads to more trustworthy results in the study of MS lesions.

REFERENCES:

[1] Tabelow, K., E. Balteau, J. Ashburner, M. Callaghan, B. Draganski, G. Helms, F. Kherif, et al. (2019) “HMRI – A Toolbox for Quantitative MRI in Neuroscience and Clinical Research.” *NeuroImage* 194:191–210; **[2]** Gracien, R.-M., A. Jurcoane, M. Wagner, S. Reitz, C. Mayer, S. Volz, S.-M. Hof, et al. (2016) “Multimodal Quantitative MRI Assessment of Cortical Damage in Relapsing-Remitting Multiple Sclerosis: Cortical Quantitative MRI in RRMS.” 44(6):1600–1607; **[3]** Gracien, R.-M., S. Reitz, S.-M. Hof, V. Fleischer, H. Zimmermann, A. Droby, H. Steinmetz, F. Zipp, R. Deichmann, and J. Klein. (2016) “Assessment of Cortical Damage in Early Multiple Sclerosis with Quantitative T2 Relaxometry: Cortical T 2 in Early Multiple Sclerosis.” *NMR in Biomedicine* 29(4):444–50; **[4]** Lommers, E., J. Simon, G. Reuter, G. Delrue, D. Dive, C. Degueldre, E. Balteau, C. Phillips, and P. Maquet. (2019) “Multiparameter MRI Quantification of Microstructural Tissue Alterations in Multiple Sclerosis.” *NeuroImage: Clinical* 23:101879; **[5]** Schmidt, P., C. Gaser, M. Arsic, D. Buck, A. Förschler, A. Berthele, M.Hoshi, et al. (2012) “An Automated Tool for Detection of FLAIR-Hyperintense White-Matter Lesions in Multiple Sclerosis.” *NeuroImage* 59(4):3774–83; **[6]** Ashburner, J., and K. Friston. (2005) “Unified Segmentation.” *NeuroImage* 26(3):839–51. **[7]** Phillips, C., Lommers, E., Pernet, C., (2017) "Unifying lesion masking and tissue probability maps for improved segmentation and normalization." In: Poster, 23rd Annu. Meet. Organ. Hum. Brain Mapping, Vancouver, Canada. **[8]** Seewann, A., E.- J. Kooi, S. D. Roosendaal, P. J. W. Pouwels, M. P. Wattjes, P. van der Valk, F. Barkhof, C. H. Polman, and J. J. G. Geurts. (2012) “Postmortem Verification of MS Cortical Lesion Detection with 3D DIR.” *Neurology* 78(5):302–8